Supercatastrophic Disruption of Asteroids in the Context of *SOHO* Comet, Fireball, and Meteor Observations

Paul Wiegert[1,2] , Peter Brown[1,2] , Petr Pokorný[3,4] , Quanzhi Ye[5] , Cole Gregg[1], Karina Lenartowicz[1],
Zbigniew Krzeminski[1], and David Clark[2,6]

[1] Department of Physics and Astronomy, The University of Western Ontario, London, Canada; pwiegert@uwo.ca
[2] Institute for Earth and Space Exploration (IESX), The University of Western Ontario, London, Canada
[3] Department of Physics, The Catholic University of America, Washington, DC 20064, USA
[4] Astrophysics Science Division, NASA Goddard Space Flight Center, Greenbelt, MD 20771, USA
[5] Department of Astronomy, University of Maryland, College Park, MD 20742, USA
[6] Department of Earth Sciences, The University of Western Ontario, London, Canada

Abstract

Granvik et al. reported an absence of asteroids on orbits with perihelia near the Sun that they attribute to the "supercatastrophic disruption" of these bodies. Here we investigate whether there is evidence for this process among other bodies with similarly low perihelia: near-Earth asteroids, *Solar and Heliospheric Observatory* (*SOHO*) comets, and meter- and millimeter-sized meteoroids. We determine that no known near-Earth asteroids have past (last 10^4 yr) histories residing significantly inside the Granvik et al. limit, indirectly supporting the disruption hypothesis. The exception is asteroid (467372) 2004 LG, which spent 2500 yr within this limit and thus presents a challenge to that theory. Phaethon has a perihelion distance hovering just above the limit and may be undergoing slow disruption, which may be the source of its dust complex. We find that the rate at which ungrouped *SOHO* comets are observed is consistent with expected rates for the injection of small (25 m) class asteroids into the near-Sun region and suggest that this fraction of the *SOHO*-observed comet population may in fact be asteroidal in origin. We also find that there is an absence of meter-sized bodies with near-Sun perihelia but an excess of millimeter-sized meteoroids. This implies that if near-Sun asteroids disrupt, they do not simply fragment into meter-sized chunks but ultimately disintegrate into millimeter-sized particles. We propose that the disruption of near-Sun asteroids, as well as the anomalous brightening and destruction processes that affect *SOHO* comets, occur through meteoroid erosion, that is, the removal of material through impacts by high-speed near-Sun meteoroids.

Unified Astronomy Thesaurus concepts: Solar system (1528); Meteoroids (1040); Near-Earth objects (1092); Comets (280); Kreutz Sungrazers (890); Asteroids (72)

1. Introduction

It has been known for some time that near-Earth asteroids (NEAs) are lost largely to orbital evolution, resulting in their falling into the Sun (Farinella et al. 1994; Gladman et al. 1997). However, it has recently been reported that asteroids may be destroyed even when their perihelia are substantially above the solar surface and their temperatures remain below that needed to melt/vaporize them. On the basis of an absence of known NEAs with small perihelia, even after painstaking removal of observational selection effects, Granvik et al. (2016, hereafter G16) concluded that asteroids undergo "supercatastrophic disruption" (SCD) when their perihelia q reach values below about 16 solar radii $R_\odot$ (or 0.074 au), with some dependence on asteroid size. Their analysis determined that neither tidal effects nor thermal melting/vaporization can adequately account for the destruction of these asteroids. No physical mechanism was proposed, but G16 speculated that the breakup may be due to thermal cracking, spin-up beyond the asteroids' cohesive strength, or explosive fracturing due to subsurface volatile release.

Here we examine the near-Sun population across a range of sizes to look for clues to the SCD process. The known near-Sun asteroids, in particular their past dynamical history; the *Solar and Heliospheric Observatory* (*SOHO*) comets; and meter-sized fireballs and millimeter-sized meteors from the near-Sun region all carry information that may be relevant to the SCD

process. First, we note that it is not clear that the SCD process is distinct from the processes of what we will refer to here as "ordinary" cometary activity and/or "ordinary" cometary fragmentation. Though the process must result in the destruction of asteroids, which may not have much ice content, it is possible that SCD may look very much like ordinary cometary fragmentation. It is even possible that after one or a few perihelion passages near the Sun, the inner volatiles are exposed by some process, and the "asteroid" becomes what is —for all intents and purposes—an ordinary comet, even displaying cometary activity when relatively far from the Sun. Thus, bodies currently labeled as "comets" with low perihelia (*SOHO* comets, for example) may in fact be undergoing SCD. In particular, we note that since the Granvik et al. (2018) NEA model includes a Jupiter-family comet (JFC) source, it would seem that JFCs likely undergo SCD either by the same or a similar process as asteroids do, because they must be driven to the near-Sun region by similar dynamical processes but do not survive there. Thus, comets are not necessarily immune from SCD. That being said, comets do undergo splitting far from the Sun as well. Over 40 split comets were reviewed by Boenhardt (2004). For none except Shoemaker–Levy 9 (which was tidally disrupted by a close approach to Jupiter) is the mechanism well understood, and some were thought to have split at heliocentric distances beyond 50 au. Thus, while comets may be vulnerable to SCD, it is in addition to other disruption processes.

In the next section, we will review the known populations of low-perihelion bodies in the context of SCD.

2. The Near-Sun Populations

2.1. Near-Sun Asteroids

The current distribution of perihelion distances of near-Sun asteroids shows a deficit near the Sun (Granvik et al. 2016), but there are many asteroids with q near this limit that might have been closer to the Sun in the past. That is because the same dynamical effects that drive asteroid perihelia into the near-Sun region can also draw them out again, if the asteroids survive. Thus, the current population of asteroids contains some asteroids that were at lower q in the past and thus potentially provide tests of and information on the SCD phenomenon.

To perform a preliminary investigation, we select all of the asteroids listed on the NeoDys website[7] that have a perihelion distance q less that 0.5 au with absolute magnitude $H < 19$ and whose orbit condition code U is greater than or equal to 2 according to JPL.[8] The quantity U runs from zero to nine and reflects how well the orbit is known, with zero indicating little uncertainty and nine indicating high uncertainty.[9] The resulting sample contains the largest NEA (diameters above 500 m, depending on albedo) at these perihelia and has the best-determined orbits.

The nominal orbits of these bodies are integrated backward for 10,000 yr within a solar system with eight planets (using the Earth–Moon barycenter for the Earth) and post-Newtonian relativistic corrections with the RADAU (Everhart 1985) integrator with an error tolerance of 10^{-12}. During the integration, passages within the G16 limit for asteroids of this size (0.06 au) are checked for. This is not an exhaustive examination of the NEA population; our sample contains only 1324 of the 19,771 objects on the NeoDys list but is intended to capture the best-known orbits most likely to have crossed the G16 limit in the past. A full study of the entire NEA population for past crossings of the G16 limit would be interesting but beyond the scope of this paper.

Though a number of our sample asteroids approach or barely cross the G16 limit—e.g., asteroid (511600) 2015 AZ$_{245}$ had $q = 0.058$ au about 4600 yr in the past—the vast majority of asteroids we examined remain outside the limit during the interval examined. This strengthens the case for SCD: if many large asteroids had survived extended periods with perihelia inside the G16 limit, it might point to the current deficit being a statistical fluke.

There is an exception: asteroid (467372) 2004 LG (which has a semimajor axis $a = 2.06$ au, eccentricity $e = 0.897$, and inclination $i = 71°$) reached $q = 0.026$ au about 2400 yr ago, half the SCD limit at its size ($H = 18.0$) and half that of any other asteroid in our sample. It spent approximately 2500 yr within $16\,R_\odot$. We repeated this simulation with 100 clones of (467372) generated from its NeoDys covariance matrix, and all showed the same behavior, so this is not simply the result of a poorly determined orbit. Asteroid (467372) 2004 LG is currently outside the G16 limit at $q = 0.21$ au and an inclination $i = 71°$. This highly inclined orbit, together with a Tisserand parameter with respect to Jupiter of 2.7, suggests

that this body may in fact be a dynamically highly evolved comet, though no activity from it has yet been reported. The past extremely low perihelion distance was previously noted by Vokrouhlický & Nesvorný (2012), who computed that the surface of the asteroid could have reached 2500 K. They assessed the effects of the denser solar wind, circumsolar dust, and the Yarkovsky effect on the orbit of 2004 LG and found them to be negligible, so there is no obvious dynamical mechanism (unless the object does at times exhibit cometary outgassing) that would have prevented it reaching a very low perihelion distance.

There are no spectra of (467372) 2004 LG of which we are aware. From NEOWISE, its diameter is 0.864 km ($H = 18.0$), and its albedo is 0.146 (Mainzer et al. 2011). The relatively high albedo makes it more likely to be an S-type than a C-type (Chapman et al. 1975; Tedesco et al. 1989; Masiero et al. 2011). Because S-types are associated with ordinary chondrites (e.g., Britt et al. 1992), this could explain its survival, as a stony composition might be more resistant to a variety of destructive processes than a carbonaceous one. The NEO model of Granvik et al. (2018) gives a probability of zero of a JFC origin, with the 3:1 resonance the most likely source (probability 0.33); thus, (467372) is dynamically likely to be asteroidal.

To help determine if (467372) 2004 LG might indeed be a comet, we conducted an archival search for images of it using the Solar System Object Image Search tool (Gwyn et al. 2012) at the Canadian Astronomy Data Centre but without success. We also obtained five unfiltered 300 s exposures tracked at the expected sky motion of (467372) 2004 LG on 2019 May 11 with the 0.61 m T24 telescope on the itelescope.net network. The asteroid was approaching the Sun at a heliocentric distance of 1.11 au at a phase angle of 62° with a JPL-predicted apparent magnitude of 19.9. The asteroid elevation was 45°, and the Moon was below the horizon. The asteroid was visible in the stacked image at 1σ at an apparent magnitude of 20.4, but no cometary activity was detectable. Pan-STARRS images of this asteroid taken in 2010 June (R. J. Weryk 2019, private communication) show an FWHM perpendicular to the trail of $1.''7$, nominally larger than that of the stars ($1.''46 \pm 0.''05$), but it was not reported as cometary at the time, nor have any of the over 100 observations listed at the Minor Planet Center as of 2019 May 27 mentioned activity as far as we are aware. At the moment, it is unclear if (467372) 2004 LG is asteroidal or cometary, but it presents a challenge to the SCD hypothesis.
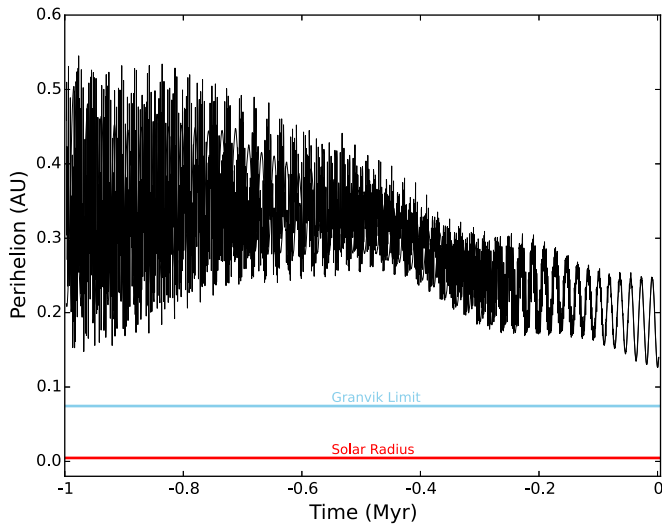
2.1.1. Phaethon

Asteroid (3200) Phaethon ($a = 1.27$ au, $e = 0.89$, $i = 22°.3$) has a perihelion distance of 0.14 au, low but outside the G16 limit. Unlike most asteroids, it is a known dust producer. It is recognized as the parent of the Geminid meteor shower (Whipple 1983) and has been seen to produce dust (though not at cometary levels) when passing perihelion (Jewitt & Li 2010). One could ask if Phaethon's dust production is due to dynamical changes in its perihelion distance: if it were at lower perihelion in the past, perhaps even inside the G16 limit for some time, this might provide a clue as to the nature of the supercatastrophic disruption process. Simulations of the orbit of Phaethon during the past million years show that its orbit has remained near but just above the 0.16 au G16 limit (see Figure 1). Thus, Phaethon may represent a boundary case, where its perihelion hovers above the supercatastrophic

Figure 1. Past evolution of the perihelion distance of (3200) Phaethon and 100 clones distributed within the orbital determination errors. The orbit is well known, so all clones remain on very similar orbits. The perihelion distance fluctuates, remaining near the G16 limit but not crossing it.

disruption limit for long times without crossing it. The dust production from Phaethon may then be the result of super-catastrophic disruption in slow motion.

From the aforementioned simulations, we conclude that the past dynamical history of the near-Sun asteroids is broadly consistent with a removal/destruction process acting at small perihelion corresponding to the G16 limit.

2.2. Near-Sun Comets

If any of the current population of periodic low-perihelion comets is in fact an asteroid in the process of SCD, then it should be on an orbit consistent with an asteroid belt origin, that is, a short-period or Jupiter-family orbit rather than Halley-type. On the JPL comet list,[10] there are only 10 short-period (<20 yr) comets listed with $q < 0.3$ au, and they are all *SOHO*-discovered comets, with the exception of 96P/Machholz. Though the process of determining these orbits and linking successive apparitions of *SOHO* comets is a difficult one, it is interesting that seven of these 10 comets (1) are ungrouped and (2) have orbits with inclinations of less than 25° (Table 1). So we have several good *SOHO* comet orbits consistent with an asteroidal or JFC origin and thus with supercatastrophically disrupting asteroids. Given that our sample of potentially supercatastrophically disrupting asteroids consists almost exclusively of *SOHO* comets, we will defer a more detailed discussion of them to the following section, where the entire *SOHO* sample, not just those with the best-determined orbits, is examined.

2.3. SOHO *Comets*

SOHO's Large Angle Spectrometric Coronagraph (LASCO) has been observing comets in the near-Sun region since 1996. Over 3000 comets, most passing within the G16 limit, have been observed, and this sample may include supercatastrophically disrupting asteroids. Lamy et al. (2013) is the last comprehensive analysis of this sample, while Jones et al. (2018) provided a useful overview of near-Sun comets: a brief

review of the relevant orbital details follows. Below, we will adopt the terminology proposed by Knight & Walsh (2013), where comets passing within the Sun's fluid Roche lobe are labeled "sungrazers," while those passing further out are "sunskirters." Because the vast majority of these comets are only seen at a single perihelion passage, their semimajor axis and eccentricity are unknown in almost all cases, though their perihelion distance and inclination can be measured.

2.3.1. Sungrazers—Kreutz Group

These have perihelia around 2 $R_\odot$, and because of their inclination i and large semimajor axis a (e.g., $i \approx 144°$ and $a \approx 64$ au for the Great March Comet of 1843–1843 D1), they originate from the Oort cloud (Biesecker et al. 2002). Most do not survive perihelion passage though larger ones, e.g., C/2011 W3 (Lovejoy), may (Kreutz 1891 as cited in Marsden 1967), and searches for them away from perihelion have been unsuccessful to date (Ye et al. 2014). Here we will take the sungrazer family to have originated from traditional cometary activity and/or fragmentation because of its retrograde inclination and large semimajor axis.

2.3.2. Sunskirters—Meyer Group

These comets have perihelia from 6 to 9 $R_\odot$ and high inclination ($i \approx 72°$; Sekanina & Chodas 2005). Many survive perihelion, at least briefly. Sekanina & Chodas (2005) considered them to be on a large aphelion orbit because arrivals are not clustered in time, suggesting a long orbital period, but neither their orbital period nor a potential parent body is known. We will consider them to be traditional cometary in nature because of their apparent large aphelion and inclination.

2.3.3. Sunskirters—Marsden and Kracht Groups (Machholz Group)

These comets have perihelia near 10 $R_\odot$ and inclinations of 10°–35° (Lamy et al. 2013). These comets typically survive their perihelion passage, though no *SOHO*-discovered members have been seen by other telescopes. These comets are part of a group dynamically associated with 96P/Machholz 1 (Sekanina & Chodas 2005; Lamy et al. 2013) that includes 2003 EH₁ (an asteroid associated with the Quadrantids meteor shower; Jenniskens 2004; Wiegert & Brown 2005). The Machholz complex is also associated with eight meteor showers at the Earth (e.g., Abedin et al. 2018). The members of this group likely split from each other, but is this traditional cometary splitting or SCD?

Sunskirting comets appear "stellar" in *SOHO* images. Lamy et al. (2013) reported that only seven have short tails in their sample of 238. Sekanina & Chodas (2005) estimated that they are nearly inert objects that only survive one or two orbits, though brighter ones may survive longer. Lamy et al. (2013) concluded that they are unlikely to be bare nuclei, however, as the amount of reflected light corresponds to a cross section of 10–100 km, unrealistically large compared to the estimated fragment size, which is orders of magnitude smaller (meters to tens of meters).

These comets could be an example of an SCD-produced family of fragments, despite their origin from a JFC; the NEO model of Granvik et al. (2018) includes a JFC source, and bodies, i.e., comets originating from that source, presumably need to undergo SCD as well, though this is not detailed in that

---

[10] ssd.jpl.nasa.gov/dat/ELEMENTS.COMET, retrieved on 2019 March 23.

Table 1
The Best-determined Near-Sun ($q < 0.3$ au) Comet Orbits from JPL

Name	Orbital Elements						Source Region Probabilities							Group
	q	a	e	i	Ω	ω	ν_6	5:2	2:1	Hun	3:1	Pho	JFC	
321P	0.047	2.43	0.980	19.7	165	172	0.09	0.00	0.00	0.01	0.87	0.00	0.03	Ungrouped
322P	0.054	2.52	0.979	12.6	0	49	0.10	0.00	0.00	0.01	0.81	0.00	0.08	Ungrouped (Kracht II)
323P	0.048	2.61	0.982	6.5	322	355	0.04	0.00	0.02	0.00	0.25	0.00	0.70	Ungrouped
342P	0.053	3.04	0.983	13.3	43	59	0.00	0.00	0.04	0.00	0.09	0.00	0.86	Ungrouped
96P	0.124	3.03	0.959	58.5	94	15	0.02	0.32	0.33	0.00	0.20	0.02	0.11	Machholz
P/1999 J6	0.049	3.10	0.984	26.6	82	22	0.00	0.00	0.08	0.00	0.12	0.00	0.79	Machholz (Marsden)
C/2002 R5	0.047	3.22	0.985	14.1	13	46	0.00	0.00	0.18	0.00	0.05	0.00	0.77	Ungrouped (Kracht II)
P/2002 S7	0.049	3.22	0.985	13.6	50	52	0.00	0.00	0.18	0.00	0.05	0.00	0.77	Ungrouped
P/2008 Y12	0.065	3.08	0.979	23.3	313	147	0.00	0.01	0.05	0.01	0.25	0.00	0.69	Ungrouped
C/2015 D1	0.028	4.94	0.994	69.6	96	235	...	...	...	...	...	...	...	Ungrouped

Note. Units of q and a are in astronomical units, and angular elements are in degrees. The final column provides the near-Sun comet group. The seven columns just prior to that one give the probabilities of their source regions being the ν_6, the 5:2 or 2:1 resonances, the Hungarias, the 3:1 resonance, the Phocaeas, or the Jupiter family of comets, according to the Granvik et al. (2018) NEO model. None of the comets have known H magnitudes, except for 96P (where $H \approx 15$), so these values are taken from the smallest size bin ($H \in [24.75{-}25.0]$). The orbital elements of C/2015 D1 (*SOHO*) are outside the region for which source probabilities are given by Granvik et al. (2018). Hui et al.'s (2015) orbit computation for C/2015 D1 differs somewhat from JPL's and indicates that it may in fact be a long-period comet.

reference. We note that 96P has only a 0.11 probability of originating from the JFC source in the Granvik et al. (2018) dynamical model (see Table 1), despite being a JFC itself (though an atypical one because of its low q and high i). Another point supporting the SCD origin of this group is the fact that it contains a large (inactive) asteroid, (196256) 2003 EH$_1$ ($a = 3.12$ au, $e = 0.619$, $i = 70°.8$, which also has a Granvik et al. 2018 probability of a JFC origin of only 0.11), and the smaller members seen by *SOHO* might be small asteroids undergoing SCD.

Arguably, the disintegration of 96P into the Machholz complex might be an expression of SCD, particularly since the primary members, 96P and (196256) 2003 EH$_1$, are dynamically unlikely to have a JFC origin according to Granvik et al. (2018). However, given the distinctly cometary nature of 96P, the largest member of this group (6.4 km diameter (Lamy et al. 2004), corresponding to $H \approx 15$ for a typical low-albedo comet, versus 2–3 km for (196256) 2003 EH$_1$ depending on albedo; it has an absolute magnitude H of 16.2[11]), we conclude that this group is the result of traditional cometary fragmentation, though it may still inform the SCD process.

2.3.4. Ungrouped Sungrazing and Sunskirting Comets

There are 75 ungrouped *SOHO* comets reported by Lamy et al. (2013). With a wide variety of inclinations and perihelia from 0.24 to nearly 40 $R_\odot$, these are a mix of unrelated sungrazing and sunskirting comets. Like other non-Kreutz comets, these are described as being meters to tens of meters in size, having optical cross sections so high that they must be displaying comae of some sort, and many survive their perihelion passage (Lamy et al. 2013). Though the spread in inclinations suggests an Oort cloud source, there is an excess of members at low inclinations. We will suggest here that the low-inclination population of ungrouped *SOHO* comets is in fact consistent with small asteroids undergoing SCD.

Lamy et al. (2013) listed 75 ungrouped *SOHO* comets recorded between 1996 and 2008. There were 149 as of 2017 (Battams & Knight 2017; Jones et al. 2018), but few of the later ones have published orbits, so we restrict our analysis here to
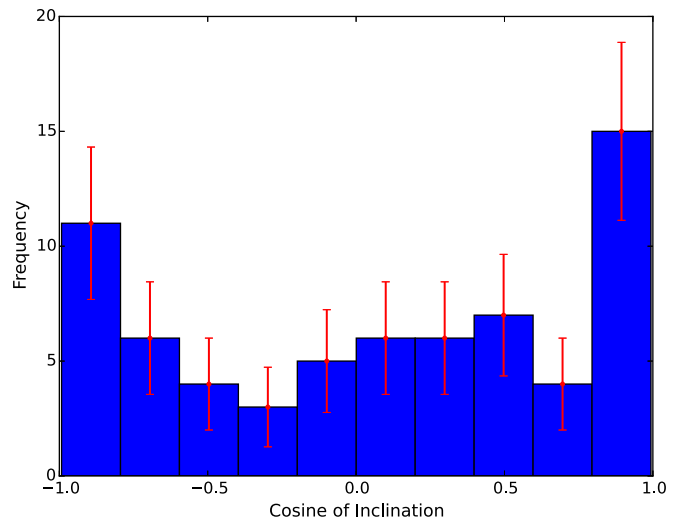
Figure 2. Distribution of cosines of the inclinations of 67 ungrouped *SOHO* comets from Lamy et al. (2013). An isotropic distribution of orbit poles, such as one originating from the Oort cloud, would have a flat distribution. The observed distribution is consistent with a spherically symmetric component plus a component concentrated in the ecliptic plane.

the Lamy et al. (2013) sample. Of the 75 with orbits, 12 were subsequently linked as multiple apparitions of comets 321P/*SOHO*, 322P/*SOHO*, 342P/*SOHO*, and C/2002 R5 (*SOHO*), leaving 67 unique comets. Three of these (C/2002 R5 (*SOHO*), C/2008 O6, C/2008 O7) and 322P are now considered a single member of the Kracht II group. The first *SOHO* comet to be observed by other instruments, 322P showed an absence of coma consistent with it being an asteroid (Knight et al. 2016). The ungrouped comets do not show much clustering in arrival time, longitude of ascending node Ω, or argument of perihelion ω and so are dynamically consistent with evolved asteroids.

Of our sample of 67, 38 have an inclination less than 90° and 29 more than 90°. A plot of the cosine of the inclinations is presented in Figure 2. If the orbits were really randomly distributed on the sphere, as one might expect for Oort cloud comets, the distribution of $\cos i$ should be flat. But there is an excess near $\cos i$ of $+1$ and -1, indicating an excess of comets in the ecliptic plane. One explanation could be an observational

bias toward comets at low inclinations. Lamy et al. (2013) discussed observational bias in the LASCO observations but did not mention biases associated with the ecliptic plane. They did mention (as did Battams & Knight 2017) that the short observational arc makes the orbit calculations difficult, with particular ambiguity in determining if the orbit is prograde versus retrograde. The plane of motion can be relatively well established, but whether the comet passes in front of or behind the Sun is much harder to determine. So we will take the excess of ungrouped *SOHO* comets in the ecliptic plane to be real and use them to calculate the rate at which they are produced for comparison with NEA models.

We can set an upper limit on the number of ungrouped comets coming from the asteroid belt by assuming that the $\cos i$ distribution of ungrouped comets consists of a uniform background of Oort cloud comets plus an excess asteroidal component. For the sake of argument, we will take the excess of comets at inclinations below 25°.8 and above 154°.2 (the first and last bins of Figure 2, since $\cos^{-1} 0.9 = 25°.8$) to be entirely asteroids moving on prograde orbits. In this case, we have ∼15 potentially supercatastrophically disrupting asteroids over our sample time frame of ∼12 yr, assuming the *SOHO* comet detection efficiency is not too far from unity, or about one per year.

If *SOHO* has been observing about one potentially super-catastrophically disrupting asteroid per year, how does this rate compare with that expected? Ye & Granvik (2019) calculated that a single asteroid of diameter greater than 0.5 km breaks up via SCD every 2000 yr. Given a power-law cumulative number distribution for small NEAs proportional to $D^{-2.7}$ (Brown et al. 2002), with D the asteroid diameter, that extrapolates to one 30 m diameter asteroid per year, consistent with *SOHO* comet size estimates of "meters to a few dozen meters" (Lamy et al. 2013).

Only a few ungrouped comets have sufficiently good orbits to use Granvik et al.'s (2018) model to determine the probability of their originating in a particular source region; these are given in Table 1. Though the JFCs are the most likely source for many of them, all show appreciable (0.2–0.8) probabilities of a main-belt origin as well.

We conclude that the ungrouped sunskirting comets are consistent with the SCD process in terms of both their rates and their orbits. Since some larger ungrouped *SOHO* comets survive at least one perihelion passage (e.g., 322P, 150–320 m diameter), while smaller ones (∼10 m) typically do not (see Table 4 in Lamy et al. 2013), this suggests a boundary between the ∼10 and ∼100 m sizes, with the smaller ones unable to survive even a single perihelion, implying that ∼10 m of material is lost per perihelion.

2.4. Meter-sized Meteoroids

Meter-sized asteroids on near-Sun orbits could either be small objects created (presumably by collisions) in the asteroid belt and driven to small q by the same processes as large asteroids, or debris from the SCD or other processes.

Here we will compare the sample of meter-class impactors observed at Earth to the NEA population near the Sun. The largest well-characterized sample of meter-sized orbits is that of Brown et al. (2016). They analyzed the orbits and in-atmosphere characteristics of 59 fireballs produced by meteoroids with preatmospheric diameters of 1 m or larger. This sample's distribution of perihelion q versus eccentricity e

is shown in Figure 3, where a deficit of bodies in the near-Sun region can be seen. The fireballs produced by impactors of this size are bright and often seen during daylight, so radiants located in the near-Sun region are not strongly biased against.

Indeed, the majority of this sample comes from US Government sensor measurements that do not show any significant day–night asymmetry.[12] The sample also includes fireballs collected by different ground-based camera networks, so it is not a completely uniform sample but is also not expected to be strongly biased against near-Sun radiants or daytime meteors. The sample is comprised mostly of asteroidal material with only a few meter-class fireballs with the characteristics of cometary material, but none were observed to have perihelia particularly near the Sun. The accuracy of individual orbital measurements from US Government sensor data has been shown to have wide variability (Devillepoix et al. 2019), but the perihelion distance tends to be among the more robust orbital elements with respect to meteor trajectory errors.

For comparison, the known NEAs are plotted in the right panel of Figure 3. The NEA catalog was downloaded from NeoDys[13] and contains 17,786 NEAs. We exclude 2015 KP$_{157}$, which has a 2 day arc with only 11 observations; its nominal q is 0.053 au but with large uncertainty. The minimum perihelion distance remaining among the NEAs is then 2005 HC$_4$, with $q = 0.07$ au.
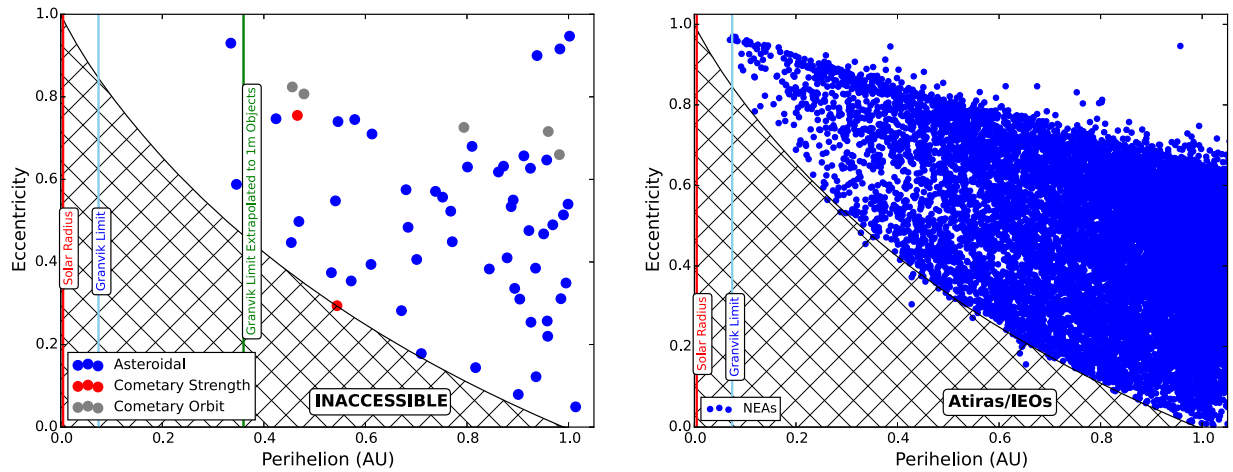
In both panels of Figure 3, the region interior to the Earth's orbit has been indicated with cross-hatching. This region is strictly unobservable in the case of fireballs, which clearly must cross Earth's orbit; for the NEAs, this region is not completely inaccessible but difficult to sample telescopically.

The NEA sample has not been debiased in Figure 3, so the two are not strictly comparable. A proper assessment of the observational effects biasing both samples would be required for a complete analysis, but we do not attempt that here. However, it is clear that the data in hand are broadly consistent with an absence of meter-sized bodies in the near-Sun region. If we extrapolate the G16 Figure 2 size dependence to meter sizes, we find that a 1 m object would not survive inside 0.36 au. This distance is indicated in Figure 3 and corresponds closely with the smallest q fireballs observed. This is an interesting clue and may indicate that the supercatastrophic process extends to even smaller sizes than G16 originally proposed, though it may simply be due to small number effects as well.

Unfortunately, there is no additional compositional information for most of these fireballs. The two with the lowest perihelion for which meteorites were recovered are Maribo ($q = 0.479$ au, a CM2 chondrite; Jopek et al. 2013) and Sutter's Mill ($q = 0.456$ au, a CM regolith breccia; Jenniskens et al. 2012). These compositions are puzzling at first glance. Because carbonaceous chondrites are weaker than the more abundant ordinary chondrites (Cotto-Figueroa et al. 2016), they should be more vulnerable to most disruption processes. It was also found by G16 that high-albedo asteroids could survive closer to the Sun than those with low albedos, but carbonaceous meteorites are associated with lower-albedo asteroids (Chapman et al. 1975; Tedesco et al. 1989; Masiero et al. 2011). In contrast to this, the bulk density of CM meteorites (2.2 g cm^{-3}; Britt et al. 2002) is lower than that of ordinary

---

[12] https://cneos.jpl.nasa.gov/fireballs/, retrieved 2019 October 3.
[13] http://newton.dm.unipi.it/~neodys2/neodys.ctc, retrieved 2018 June 6.

Figure 3. Perihelion vs. eccentricity for the 59 m class fireballs of Brown et al. (2016; left panel) and the known NEAs (right panel). The shaded area indicates orbits that are entirely inside the Earth's (interior-Earth objects (IEOs), or Atiras). The G16 limit is indicated in both panels. The left panel also includes an extrapolation of the G16 to meter sizes, which corresponds closely to the lowest perihelion fireballs so far observed.

chondrites (3.6–3.9 g cm^{-3}), achondrites (3.2 g cm^{-3}), and other carbonaceous chondrites except CI (2.1 g cm^{-3}), which could allow them to better survive thermally driven destruction processes.

However, the fact that our two lowest-q meteorites are CMs is likely simply a result of poor statistics. (1) The three other carbonaceous meteorites with known orbits do not have low perihelia. Orgueil had $q = 0.87 \pm 0.01$ au (Gounelle et al. 2006), Murchison had $q = 0.99 \pm 0.01$ au (Halliday & McIntosh 1990), and Tagish Lake had $q = 0.891 \pm 0.009$ au (Brown et al. 2000). (2) The cosmic-ray exposure ages of Maribo (0.8–1.4 Myr; Haack et al. 2012) and Sutter's Mill (0.082 ± 0.008 Myr; Nishiizumi et al. 2014) are very young compared to carbonaceous chondrites overall (millions to tens of millions of years; Scherer & Schultz 2000), so these may well have survived simply due to their youth. (3) Sutter's Mill and Maribo were both particularly large impactors. Maribo (3.3 m diameter) had the fourth-largest initial size of any of the 59 meteorite-producing fireballs with well-measured orbits in Brown et al. (2016), while Maribo (1.1 m) was in the top one-third. These are both atypically large precursor meteoroids, which may help to explain why they could survive to such relatively small q.

Since meter-sized bodies are driven into the near-Sun region by essentially the same dynamical effects as those that drive kilometer-sized NEAs there, we conclude that meter-sized bodies supercatastrophically disrupt by processes ostensibly similar to those affecting kilometer-sized ones. This also suggests that kilometer-sized bodies do not break up into meter-sized bodies, or at least only do so temporarily before those pieces are themselves destroyed/removed. This has implications for the underlying mechanism, as some possibilities, such as tidal disruption, spin-up, explosive release of volatiles, or collision with another asteroid, would produce large fragments that are not seen. Processes that produce small fragments are thereby favored, such as thermal cracking or meteoroid bombardment.

2.5. Millimeter-sized Meteors

The sample of millimeter-sized particles coming from the near-Sun region provides information similar to the meter-sized sample but with some additional complications.

First, there are a number of known comets with perihelia in the near-Sun region and thus potentially contaminating the sample of SCD-produced asteroid meteoroids (if any). On top of this are almost certainly long-since extinct and/or disrupted comets, whose dust may remain though the parent objects are now gone. This was less of an issue for meter-sized meteoroids because comets are not important sources of these: (1) meteor showers derived from comets are not expected to contain meter-sized objects (Beech & Nikolova 1999), (2) searches for meter-sized fragments of Phaethon (Geminids shower parent and possible extinct comet) have been unsuccessful (Jewitt et al. 2019; Tabeshian et al. 2019; Ye et al. 2018), (3) nor are any such meter-sized shower members observed associated with cometary-derived meteor showers (Brown et al. 2016), with the exception of the Taurid meteor stream (Spurný et al. 2017). The cometary ejection processes driven by water sublimation are limited to lifting particles smaller than ∼10 cm from the nucleus surface (Whipple 1951; Whipple & Huebner 1976; Beech & Nikolova 1999). But millimeter-sized cometary meteors with low perihelia are common and must be carefully addressed.

Second, millimeter-sized meteoroids are subject to significant Poynting–Robertson (PR) drag. This is a relativistic effect due to the asymmetric reradiation of sunlight that causes these particles to spiral into the Sun and systematically reduces their perihelion distances; such dynamical effects must also be taken into account.

Our sample of millimeter-sized near-Sun meteors is collected with the Canadian Meteor Orbit Radar (CMOR; Webster et al. 2004; Jones et al. 2005; Brown et al. 2008). Located near London, Canada, CMOR is a backscatter radar comprising a 15 kW transmitter operating at 29.85 MHz and five separate receiver stations. Meteor echoes detected at the main site plus two or more stations produce velocity measurements of approximately 5000 meteor echoes daily. Meteoroid orbits measured by CMOR have size limits that are strongly velocity-dependent. The lower size limit for detection at 70 km s^{-1} is submillimeter to almost 5 mm at 12 km s^{-1} (Ye et al. 2016).

The advantage of a meteor radar over optical camera meteor detection is that the radar—being able to operate with equal efficiency both day and night—is not biased against the near-Sun region. Thus, our sample includes low-perihelion meteors
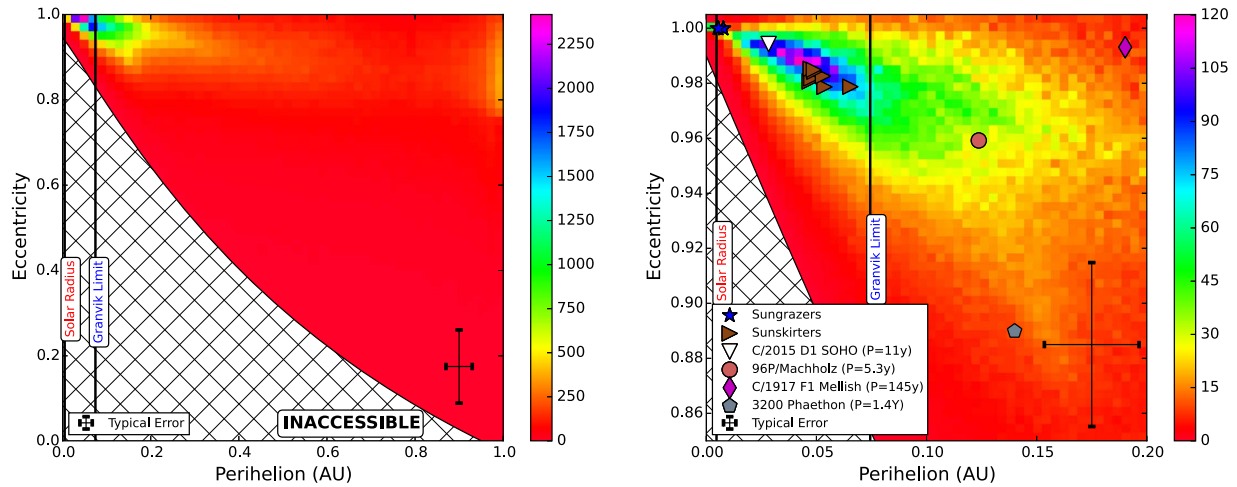
Figure 4. Debiased number of CMOR-collected meteors for all meteors with $q < 1$ au (left panel) and the near-Sun region (right panel). The G16 limit and the radius of the Sun are indicated by vertical lines. The median error bars for an individual meteor are shown at the lower right. The distribution of comets with $e < 1$ and period $P < 1000$ yr is superimposed for comparison. There is clearly a near-Sun meteor population, but much of it is cometary in origin. The hatched region cannot be sampled from Earth because these orbits do not intersect our planet.

collected both inbound to and outbound from the Sun. Figure 4 shows a density plot of the meteors collected during 2011–2019. The sample of meteors with $q < 1$ au contains 2,027,678 meteors. These represent the highest-quality meteors in the sample. They were selected because they were detected by a minimum of four of the six CMOR stations, had a consistent measured inflection pick at all stations compared to the best-fit time-of-flight velocity solution, and had an in-atmosphere time-of-flight speed within the pre-t0 speed and its uncertainties based on the hybrid KDE method described in Mazur et al. (2019). The pre-t0 speed is an independent single-station estimate of speed for specular echoes that can be used to check the time-of-flight method. Hence, when the time-of-flight speed and pre-t0 speed agree to within the uncertainty, we have high confidence in the measured speed (and trajectory).

Meteor radars measure the number of meteors passing through a particular atmospheric area; to make this comparable to the telescopic sample of asteroids, which is a volume sample, each meteor is assigned a debiasing weight inversely proportional to the collision probability of its orbit with our planet (Öpik 1951). An additional term corrects for the relative geometry of the meteor radiant and the gain pattern of the radar. This term is inversely proportional to the instantaneous effective collecting area of the radar as described in Kaiser (1960) and Brown & Jones (1995). We will refer to the meteoroid orbit sample for which these corrections have been made as the "weighted" or "debiased" sample, and it is suitable for direct comparison with the usual telescopic sample of asteroids if no size threshold is considered.

Figure 4 shows the distribution of meteoroid orbits in the inner solar system as measured by CMOR. Of the most interest to us here is the concentration of meteoroids in the upper left corner. There is undoubtedly a concentration of meteor orbits with low perihelia, and we can immediately conclude that millimeter-sized meteoroids can survive in the near-Sun region even if larger asteroids may not. But many of these meteors are cometary in origin and thus not the result of asteroidal SCD.

One can first search for signs of the SCD process by looking for near-Sun meteor showers with no known parent body. This was attempted by Ye & Granvik (2019), who found that a disrupted 0.5 km asteroid could supply such a stream.

However, they found more meteoroid streams than were compatible with the expected rate of asteroid SCD. Here instead we will look at the broad nonlocalized distribution of meteoroids consistent with the disruption of meter-class asteroids, which follow essentially the same dynamical pathways as kilometer-sized asteroids into the near-Sun region. This is motivated by the ungrouped *SOHO* comets discussed in Section 2.3.4 and the fact that the debris component (if any) of small asteroids is less subject to the vagaries of small numbers than that of kilometer-class asteroids.

Radar meteor measurements do not provide sufficient information to distinguish asteroidal from cometary meteors based on physical ablation behavior. So we are reduced to trying to disentangle cometary dust from asteroidal dust on the basis of their orbits. We will assess the existence of an "asteroidal SCD" component near the Sun by examining a restricted region of orbital space calculated to exclude (1) those regions occupied by known periodic comets over the last 10,000 yr and (2) the strong near-Sun meteor showers (which are from comets). Once we discuss how we obtain this sample, we will return to a discussion of the origin and properties of any dust found there.

2.5.1. Determining an Uncontaminated Region

Our first step examines contamination by other comets of the near-Sun region by integrating known periodic comets backward in time for 10,000 yr and then excluding any regions of phase space that they visited from our sample. This is a conservative filter, since meteoroids shed by comets evolve dynamically in much the same way as their parents, and a meteoroid ejected in the past does not remain on the orbit it was deposited on, but rather follows the parent comet roughly through phase space. Here we consider the 10 known short-period comets with $q < 0.3$ au, discussed earlier in Section 2.2 (see also Table 1). We integrate the nominal orbits with the RADAU15 Everhart (1985) algorithm with a tolerance of 10^{-12}. The influence of the Sun and eight planets is included, as are the effects of general relativity (post-Newtonian approximation). Cometary nongravitational forces are not considered; they are not well known for these comets, and though possibly strong during perihelion passage, they are
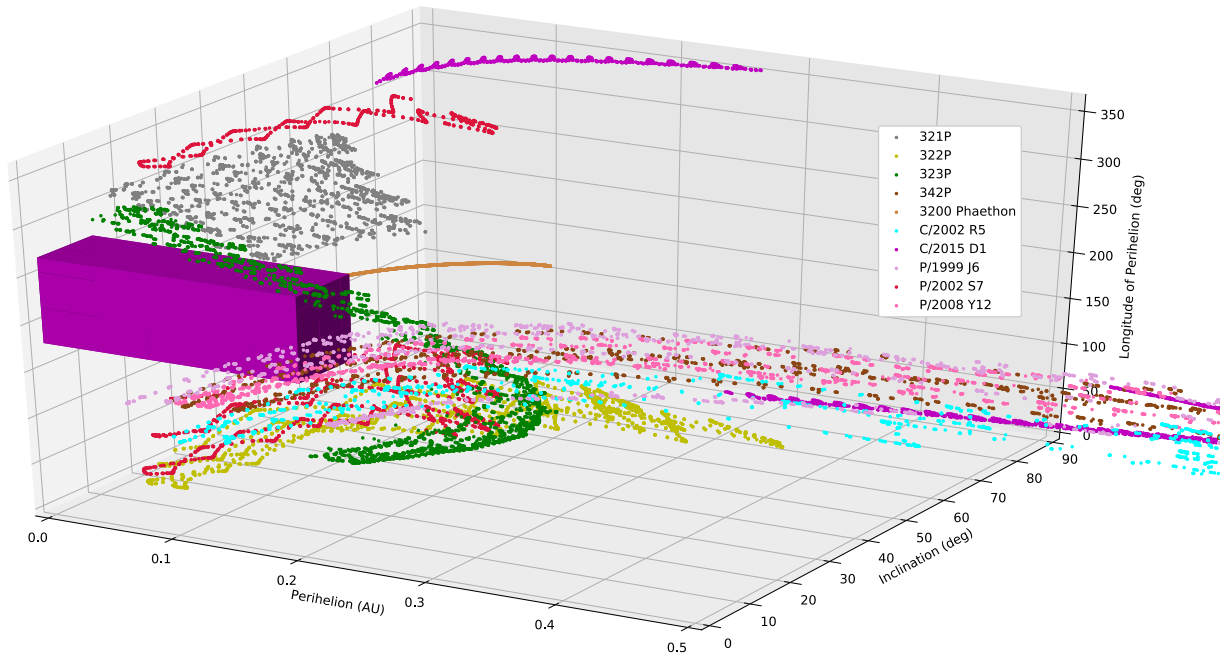
Figure 5. Past evolution of the perihelion distance q, inclination i, and longitude of perihelion ϖ for our selected comets (see Table 1) over the last 10,000 yr. Known comets move through a substantial fraction of near-Sun space during this time frame, complicating our attempts to find a region where cometary dust does not dominate. Our choice of "uncontaminated region" is shown in purple.
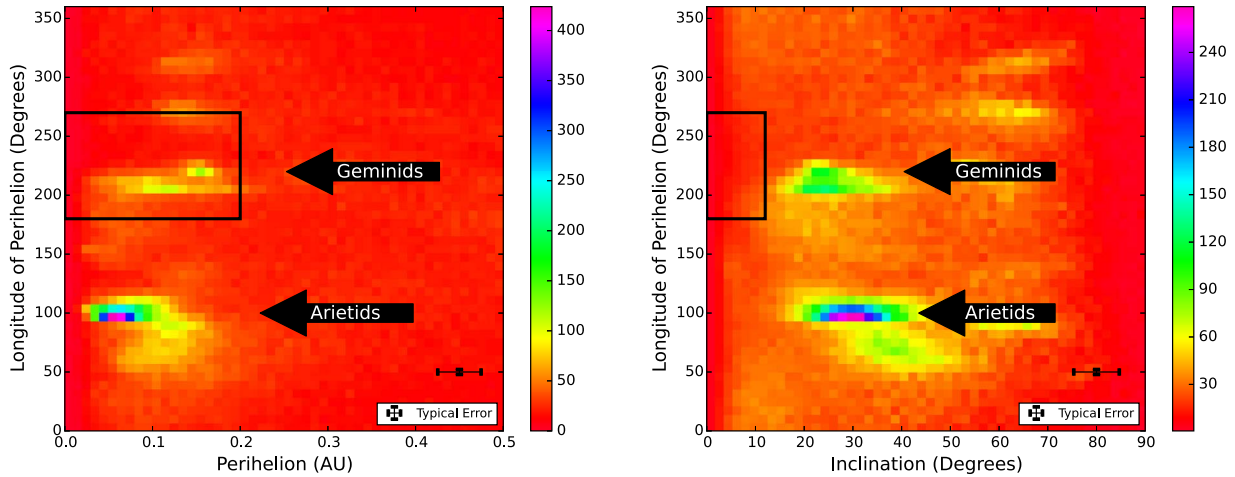
Figure 6. Debiased meteor density plot for the near-Sun region for all perihelia less than 0.5 au and inclinations less than 90°. The arrows indicate the location of two major meteor showers, the Geminids and daytime Arietids. The region of our sample, selected to avoid both contamination by known meteor showers and potential contamination by known low-perihelion comets, is indicated by the black rectangle.

short-lived and have a very short lever arm as well. Our purpose here is not to perform an exhaustive simulation of the near-Sun environment but only to avoid the most obvious sources of dust contamination. Figure 5 presents the time evolution of these comet orbits.

For our second step, we exclude the two strongest near-Sun meteor showers, the Geminids ($q = 0.137$ au, $i = 23°.2$) associated with asteroid (3200) Phaethon and the Machholz complex showers, which include the daytime Arietids ($q = 0.074$ au, $i = 30°.6$, $\varpi = 106°.7$) and north ($q = 0.096$ au, $i = 24°.8$, $\varpi = 108°.9$) and south ($q = 0.058$ au, $i = 31°.5$, $\varpi = 100°.1$) δ Aquariids. The orbital elements above are the CMOR values for these showers reported in Brown et al. (2010).

A plot of the density of CMOR meteor orbits as a function of perihelion distance q and longitude of perihelion $\varpi = \Omega + \omega$

is shown in Figure 6. Longitude of perihelion ϖ is chosen because it is more closely conserved over time than longitude of the ascending node.

Much of the near-Sun region is visited by comets in our sample (Figure 5), and there are limited choices of uncontaminated regions. Near $\varpi \sim 100°$, we see the Machholz complex comets associated with the daytime Arietids meteor shower, and the presence of this strong shower, along with associated contaminating comets (Figure 5), will lead us to exclude the region with $0° < \varpi < 180°$. The Geminids are visible near $200° < \varpi < 230°$, while the daytime Arietids and other Machholz complex meteors are at $50° < \varpi < 120°$. We can see from Figure 5 that regions with $270° < \varpi < 360°$ may have low-inclination contamination from 321P ($i = 20°$) and 323P ($i = 6°$), two small ungrouped *SOHO* comets. These are unlikely to contribute much dust because of their size, and
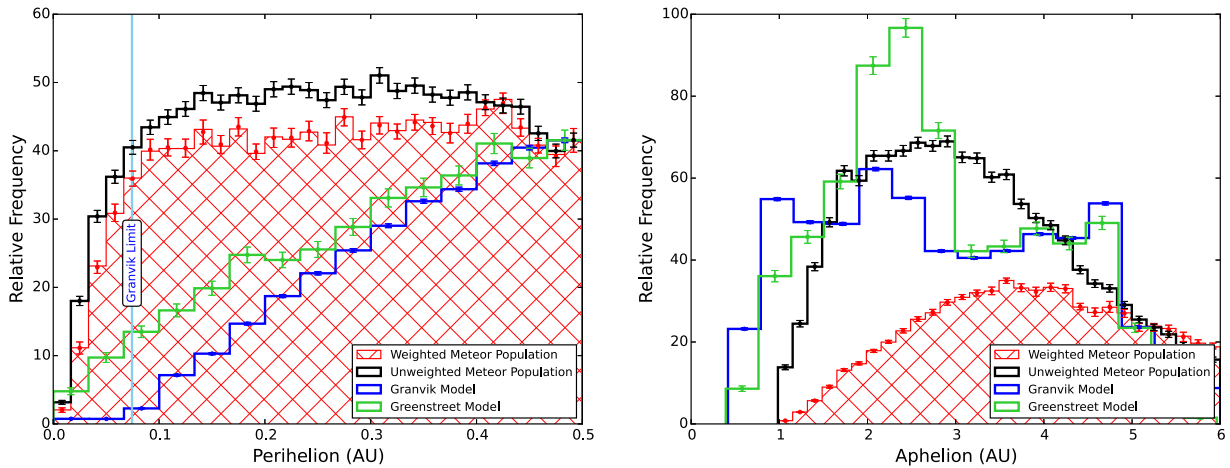
Figure 7. Perihelion and aphelion distribution for our sample of near-Sun radar meteors. The Greenstreet et al. (2012) and Granvik et al. (2018) models are included for comparison. There is an overabundance of near-Sun meteors at low perihelia compared to NEAs, including considerable material inside the G16 limit. All models are normalized to the same value at $q = 0.5$ au for perihelion distance and $Q = 5.2$ for aphelion distance.

indeed, there seems to be little dust apparent in this region of Figure 6. We will see later that these may in fact be supercatastrophically disrupting asteroids (see Section 2.3.4), but for safety, we will exclude the regions they visit. The region of $180° < \varpi < 270°$ is free of low-inclination comets but does contain Phaethon and the Geminid shower ($q = 0.137$ au, $i = 23°.2$; Brown et al. 2010). The compactness of the shower in inclination and the motion of Phaethon's dynamics suggest that we can remove Geminid contamination by excluding inclinations above 12°. Though the Geminids do not appear to create much dust at $\varpi > 230°$, to avoid creating an awkwardly shaped sample region, we will exclude $i > 12°$ across our sample.

2.5.2. Final Sample Region

The aforementioned considerations lead us to select our notionally uncontaminated region as $0° < i < 12°$, $180° < \varpi < 270°$, shown in purple in Figure 5. A histogram of the number of meteor orbits in this region is shown in Figure 7. There is definitely a population of millimeter-sized meteoroids in this region of near-Sun space.

Figure 7 tells us that millimeter-sized asteroidal meteoroids are abundant in the inner solar system. They become more abundant relative to NEAs as q decreases, and they can survive well within the G16 limit. These properties all support the hypothesis that supercatastrophically disrupting asteroids disrupt into millimeter-sized fragments, fragments that are themselves relatively resistant to the disruption process.

Extracting additional information from these orbits is difficult because (1) despite our debiasing (Section 2.5), the need for collision with the Earth imparts a complex geometrical constraint on the data, and (2) these orbits are highly evolved. We do, however, note that the material in our subsample is on orbits with aphelia Q near 4 au (see Figure 7, right panel), consistent with evolved material, either from JFCs or the main belt, that is moving inward under PR drag.

Our model of cometary contamination did not include 2P/Encke, as its perihelion distance ($q = 0.33$ au) is nominally outside the limit of 0.3 au chosen in Section 2.5.1, but could it be a contributor? Its aphelion distance Q is near 4 au (where our meteor sample peaks; Figure 7), and it is associated with the Taurid meteor shower (Whipple 1940). The inclination

($i = 11°.8$) and longitude of perihelion ($\varpi = 161°.1$) of 2P/Encke are near but outside our sample region, and Figure 6 shows little meteor activity near the location in question. We conclude that it is not a significant contributor to our sample. However, it does illustrate the difficulty in determining the origin of this material. Though we cannot categorically exclude extinct/disrupted JFCs as the source of this dust, it cannot obviously be linked to known cometary parents and is consistent with the resonant processes that drive NEAs out of the main belt and into the Sun (Farinella et al. 1994; Gladman et al. 1997).

It is worth noting that these meteoroids cannot have been put in place solely through the effects of PR drag on meteoroids produced elsewhere in the solar system. This is because PR drag, though it does cause meteoroids at these sizes to spiral in toward the Sun, also causes the eccentricity e to monotonically decrease very rapidly relative to the rate of decrease of q in our region of interest. Wyatt & Whipple (1950) provided analytic expressions for PR drag evolution and showed that particles follow

$$q = \frac{Ce^{4/5}}{1+e} \qquad (1)$$

independent of a, where $C = q_0 e_0^{-4/5}(1 + e_0)$ and q_0 and e_0 are the initial values of the perihelion and eccentricity. These produce very steep curves in our region of interest, as shown in Figure 8. As a result, PR drag is actively removing material from our sample, rather than injecting it.

Could this material be drawn into the near-Sun region by Kozai oscillations? These are caused by the long-term gravitational effects of the planets and create correlated changes in q and i so that an orbit with larger q and higher i is drawn down to an orbit with smaller q and lower i, the latter being rather like the meteoroid orbits in our sample. Figure 9 shows the lines of constant z-component of the angular momentum, which meteoroids follow under the Kozai effect. We can see qualitatively that for dust to be emplaced inside the G16 limit by Kozai oscillations, the dust must already be at (1) a low-perihelion distance at moderate (30°–60°) inclination or (2) a high (60°–90°) inclination without much constraint on q. We have already eliminated the known periodic low-perihelion comets as possible sources from our earlier analysis,
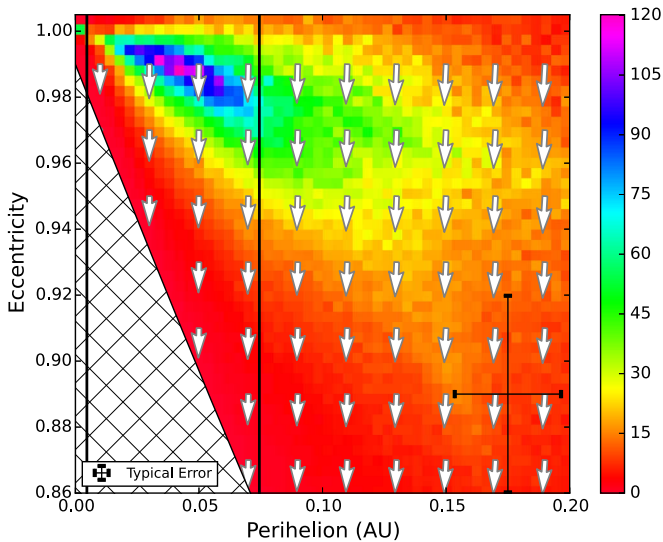
Figure 8. Near-Sun meteor distribution, with arrows indicating the direction of evolution under PR drag. The length of the arrows is proportional to the $\log_{10}$ of the magnitude of PR drag. The direction of the arrows indicates that PR drag is removing material from our sample region by circularizing their orbits faster than it decreases their perihelion distance. Median measurement errors for meteors in this sample are represented by the black bars in the bottom right part of the figure.
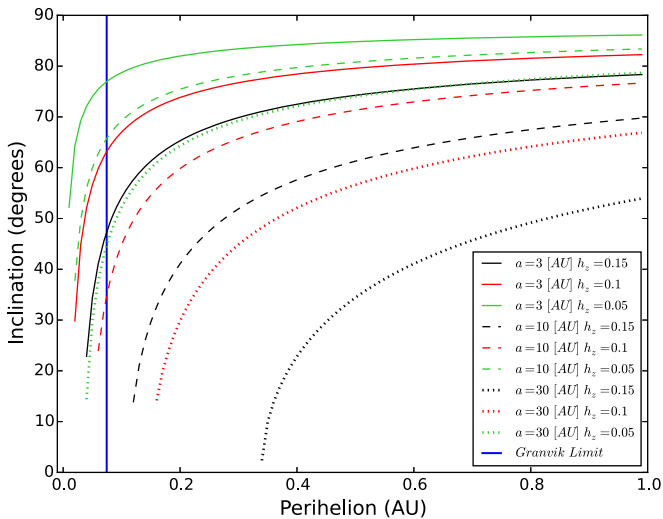
Figure 9. Lines of the constant z-component of the angular momentum $h_z = \sqrt{1 - e^2} \cos i$, indicating the paths meteoroids follow under the Kozai effect. The vertical blue line indicates the G16 limit. Lines that cross this limit indicate the possible delivery of meteoroids to near-Sun space from high-inclination comets.

so item (1) is not an issue. High-inclination periodic comets could supply this dust, and they are common, so item (2) is more difficult to eliminate as a possibility. However, high-inclination comets have orbits that are typically much larger than those of the dust observed by the meteor radar ($a \sim 2$ au), though the orbit-shrinking effects of PR drag may account for some of the difference.

So the two clearest possible sources for the dust in our sample are either relatively young dust from small super-catastrophically disrupting NEAs/JFCs being drawn into the near-Sun region by the same process that drives NEAs into the Sun (Farinella et al. 1994) or old dust from high-inclination comets that has been driven by Kozai oscillations into its

current orbit. The model of Pokorný et al. (2014) indicates that relatively little dust from Halley-type comets makes it to low-inclination, low-perihelion orbits, but there is some. A careful modeling of dust orbital evolution under the effects of PR drag and the planets would be necessary to distinguish between SCD, cometary, and Kozai-driven processes, but that is beyond the scope of this paper. Nonetheless, we conclude that there is near-Sun dust on orbits consistent with small supercatastrophi-cally disrupting asteroids, though such asteroids may not be the only possible source of such dust.

3. Meteoroid Erosion as the Cause of SCD

The cause of SCD remains unclear. It was shown by G16 that tidal effects and evaporation could not account for the process, and they suggested that thermal cracking, spin-up, and subsequent disruption or the heating of subsurface volatile pockets might provide a mechanism. Here we propose that the SCD process is produced by erosion of asteroids by near-Sun meteoroids. If this is the case, such erosion should affect both asteroids and comets in the near-Sun region, and we suggest that the anomalous brightening of near-Sun comets can also be explained by meteoroid erosion as well. Alternative explanations for the anomalous brightening of near-Sun comets includes the sublimation of olivine and pyroxene from dust grains (Kimura et al. 2002) and the onset of sublimation in a previously thermally stable component of the nucleus (Knight et al. 2010)

3.1. Phenomena that Support Meteoroid Erosion as the Cause of SCD

3.1.1. Anomalously Fast Near-Sun Brightening

The sunlight received by a body in orbit is proportional to one over the heliocentric distance r_h^2. Near-Sun comets typically brighten faster than this and faster than is typical of regular comets (which often go like r_h^{-4}; Festou et al. 1993). Knight et al.'s (2010) analysis of nearly 1000 Kreutz comets observed by *SOHO* shows a stage of rapid brightening following $r_h^{-7.3 \pm 2.0}$ from an unknown heliocentric distance (but that it is "unlikely" to be beyond $50 R_\odot$) to $24 R_\odot$, where the brightening then drops to $r_h^{-3.8 \pm 0.7}$. Hui et al. (2015) found $r_h^{-5.5}$ dependence for *SOHO* comet C/2015 D1 on its inbound leg, and Ye et al. (2014) reported on two Kreutz comets whose brightening profiles had exponents consistent with -4, while three other comets had sharper values (-7 and beyond).

The kinetic energy flux of radially infalling meteoroids goes like $r^{-3.5}$, increasing more steeply than solar illumination, and could better account for the observed rapid brightening.

3.1.2. The Universality of Kreutz Light Curves

Biesecker et al. (2002) found that Kreutz sungrazing "comets all reach a peak brightness at one of two characteristic distances (both near $12 R_\odot$) and that the comets fragment at another characteristic distance (about $7 R_\odot$)." They also said, "The similarity of the light curves is remarkable in that all reach a peak brightness at about the same heliocentric distance. In addition, the shape of the curves are also very similar." Dimming after peak brightness is reached could be accounted for by volatile depletion, perhaps, but the uncorrelated spins, shapes, sizes, inhomogeneities of composition, etc. of these

comets make universal light curves based solely on sunlight-driven volatile release unlikely at best.

However, such behavior could naturally be produced by the passage of the comets through a near-Sun meteoroid stream. If this stream was old enough to have dispersed around its orbit, all Kreutz comets passing through this portion of space would encounter a flux of high-speed particles that could release gas and dust in a consistent, repeatable manner independent of the precise properties of the surface or subsurface volatile distribution of the comet itself.

Do non-Kreutz, i.e., sunskirters, show similarly repeatable light curves? Lamy et al. (2013) said that the light curves of the sunskirters (Meyer, Marsden & Kracht = Machholz, and ungrouped) exhibit different behavior but that "this primarily results from the differences in the distance ranges in which the measurements were made." So whether the light curves of non-Kreutz comets can be as easily attributed to a coherent near-Sun meteoroid environment is less clear. They did note that the most common behavior is "a continuous increase of the brightness as the comet approaches perihelion, reaching a peak before perihelion then progressively fading." This commonality is particularly intriguing, since solar energy input must continue to increase as r_h decreases, but the meteoroid flux need not.

3.1.3. Brightening Often Diminishes Despite Moving Closer to the Sun

SOHO comets often diminish or remain constant in brightness despite continuing to approach the Sun, and this behavior shows some correlation with the comet family. Lamy et al. (2013) said "the real surprise comes from many comets (mostly from the Machholz group) with nearly "flat" light curves." This could be accounted for by inhomogeneities in the meteoroid environment, such that the meteoroid flux closer to the Sun is less than the flux further away, owing either to how the meteoroids were deposited by their parents, their subsequent dynamical evolution, or their destruction by thermal processes (Čapek & Vokrouhlický 2010) or collisions with other meteoroids.

3.2. The Characteristics of Meteoroid Erosion

Having proposed meteoroid erosion as the cause of SCD, how does it stack up to other destructive processes? The speed of a meteoroid on a nearly circular orbit near the Sun is

$$v \approx 134 \left(\frac{r_h}{10 \, R_\odot} \right)^{-1/2} \, \text{km s}^{-1}. \qquad (2)$$

At a distance of $r_h = 10 \, R_\odot = 0.0465$ au, a 6 mm diameter meteoroid (density $1000 \, \text{kg m}^{-3}$) on a retrograde circular orbit encountering a prograde asteroid deposits a kinetic energy of about 1 MJ, equal to that of a stick of dynamite.[14] Retrograde meteor orbits (originating from Oort cloud comets) are abundant at the Earth and spiral into the Sun through PR drag, though meteoroids on less extreme orbits may provide erosive impacts of reduced but similar energies. There is no question that high-speed meteoroid impacts are physically able to remove material from and eventually destroy asteroids if present in sufficient numbers. But are there enough of them?

Unfortunately, Earth-based meteor radars or cameras cannot measure the true near-Sun meteoroid population; they can only detect those that remain on highly elongated orbits. However, the circularization and inspiraling of meteoroid orbits through PR drag means that there is likely a substantial population of near-Sun meteoroids continually being fed into the near-Sun region. Dynamical models of these are starting to be constructed (e.g., Pokorný et al. 2018), though these regions are largely inaccessible to meteor measurement techniques at Earth.

Wiegert (2015) studied the effect of meteoroids as a source of drag on the asteroidal population near the Earth, and we extrapolate that model to the near-Sun region to assess the meteoroid impact rate on near-Sun objects. The flux of meteoroids onto an asteroid on a circular orbit at $r_h = 1$ au was estimated at $3 \times 10^{-8} \, \text{m}^{-2} \, \text{s}^{-1}$ (about one impact per year per square meter) at a meteoroid mass of $1.5 \times 10^{-8} \, \text{kg}$ (300 μm diameter at a density of $1000 \, \text{kg m}^{-3}$). The dynamical evolution of such dust from the Earth to the near-Sun region is complex, but if we assume for simplicity that it is mostly on nearly radial orbits (the near-Earth dust complex is known to be dominated by the helion and antihelion sporadic meteor sources that contain just such radial orbits; Jones & Brown 1993), then the number of impacts will scale like $r_h^{-2.5}$ (-2 for simple geometry with an additional 0.5 for the $r_h^{-0.5}$ speed dependence), or by a factor of ≈ 1800 at $10 \, R_\odot$. The 300 μm meteoroid mentioned earlier carries a kinetic energy of 400 J at $10 \, R_\odot$, comparable to a bullet fired from a handgun, and our target asteroid is hit several times per day per square meter.

Whether this is sufficient to provide for the erosion necessary to produce the disruption of asteroids on its own is unclear but seems promising. In addition to direct removal, impacts could uncover fresher, more volatile-rich material; for example, there is evidence that lunar meteoroid impacts must exceed a certain energy before they can release water from the surface, owing to a desiccated layer several centimeters deep (Benna et al. 2019). The speed and number of meteoroids near the Sun could cause the cracking of an object's low thermal conductivity mantle with subsequent bursts of released volatiles.

In Section 2.3.4 it was noted that the fact that small *SOHO* comets do not survive even a single perihelion passage may require the removal of several meters of material from their surfaces during the few days spent in the near-Sun region, and the impact rate computed above may not be sufficient to do so. The disruption of a stable low thermal conductivity mantle resulting in subsurface volatile exposure to sunlight could be highly destructive, but the effects of high-speed impacts into loose regolith are not known. However, given the order of magnitude of the effect of meteoroid erosion, it seems likely to be an important contributor to the destruction of near-Sun asteroids.

4. Conclusions

The process of disruption of near-Sun comets has been examined in the context of the known NEAs, *SOHO* comets, and meteoroid populations at different sizes.

The past dynamical history of known NEAs is supportive of the SCD hypothesis in that there are not many known NEAs that have spent time within the G16 limit. The exception is (467372) 2004 LG, which spent 2500 yr within that limit and survived, having now evolved to a larger perihelion. Phaethon

---

[14] https://www.chemistryviews.org/details/ezine/3622oid371/145_Years_of_Dynamite.html

may represent a curious boundary case, in that its perihelion remains near but does not cross the G16 limit.

SOHO comets inform the study of SCD, but most *SOHO* comet families (Kreutz, Meyer, and Machholz) are better described as originating from ordinary comet fragmentation than SCD. The exceptions are the ungrouped *SOHO* comets, which have an excess of orbits in the ecliptic plane consistent with the rate at which small NEAs are expected to be injected into this region. Thus, these latter comets may in fact be asteroidal in nature, and additional study of this possibility is recommended.

There is an absence of meter-class fireballs seen with perihelia in the near-Sun region, but a population of millimeter-sized meteoroids (that may be but are not obviously cometary) extends well inside the G16 limit. This suggests that asteroids do not disrupt into meter-sized pieces but may break up into smaller ones. The recovered meteorites with the two lowest known perihelia are relatively fragile, low bulk density, low-albedo carbonaceous chondrites, though whether any of these features are clues to the SCD process or simply coincidence is not yet clear.

We propose that the supercatastrophic disruption of near-Sun asteroids is due to meteoroid erosion. Though the population of near-Sun meteoroids is unknown, extrapolation from the Earth indicates that high-energy meteoroid impacts occur frequently on and deliver considerable energy to near-Sun bodies. Meteoroid impacts could also reproduce some of the puzzling brightening features seen in *SOHO* comets. The supercatastrophic disruption of asteroids due to meteoroid impact could include direct removal of material by cratering ("sandblasting"), the exposure of subsurface volatiles by mantle removal, and fracturing into several pieces.

Testing of the meteoroid erosion hypothesis and distinguishing it from competing processes will not be easy. The careful analysis of the size distribution of near-Sun meteoroids is one possible approach, since the resultant size distribution is likely to be different for different processes. Other meteoroid impact/erosion processes in the solar system, such as the particle ejection events from asteroid (101955) Bennu (Lauretta et al. 2019), are also likely to provide valuable clues. Ultimately, reliable measurements and/or models of the near-Sun meteoroid environment will be needed to assess the true importance of meteoroid impacts on bodies traveling through this region.

ORCID iDs

Paul Wiegert https://orcid.org/0000-0002-1914-5352
Peter Brown https://orcid.org/0000-0001-6130-7039
Petr Pokorný https://orcid.org/0000-0002-5667-9337
Quanzhi Ye https://orcid.org/0000-0002-4838-7676
David Clark https://orcid.org/0000-0002-1203-764X

References

Abedin, A., Wiegert, P., Janches, D., et al. 2018, Icar, 300, 360
Battams, K., & Knight, M. M. 2017, RSPTA, 375, 20160257
Beech, M., & Nikolova, S. 1999, MNRAS, 305, 253
Benna, M., Hurley, D. M., Stubbs, T. J., Mahaffy, P. R., & Elphic, R. C. 2019, NatGe, 12, 333
Biesecker, D. A., Lamy, P., Cyr, O. C., St., Llebaria, A., & Howard, R. A. 2002, Icar, 157, 323
Boenhardt, H. 2004, in Comets II, ed. M. Festou, H. U. Keller, & H. A. Weaver, Jr. (Tucson: Univ. Arizona Press), 301
Britt, D. T., Tholen, D. J., Bell, J. F., & Pieters, C. M. 1992, Icar, 99, 153
Britt, D. T., Yeomans, D., Housen, K., & Consolmagno, G. 2002, in Asteroids III, ed. W. F. Bottke, Jr., A. Cellino, P. Paolicchi, & R. P. Binzel (Tucson, AZ: Univ. Arizona Press), 485
Brown, P., Spalding, R. E., ReVelle, D. O., Tagliaferri, E., & Worden, S. P. 2002, Natur, 420, 294
Brown, P., Wiegert, P., Clark, D., & Tagliaferri, E. 2016, Icar, 266, 96
Brown, P., Wong, D. K., Weryk, R. J., & Wiegert, P. 2010, Icar, 207, 66
Brown, P. G., Hildebrand, A. R., Zolensky, M. E., et al. 2000, Sci, 290, 320
Brown, P. G., & Jones, J. 1995, EM&P, 68, 223
Brown, P. G., Weryk, R., Wong, D., & Jones, J. 2008, Icar, 195, 317
Chapman, C. R., Morrison, D., & Zellner, B. 1975, Icar, 25, 104
Cotto-Figueroa, D., Asphaug, E., Garvie, L. A., et al. 2016, Icar, 277, 73
Čapek, D., & Vokrouhlický, D. 2010, A&A, 519, A75
Devillepoix, H. A. R., Bland, P. A., Sansom, E. K., et al. 2019, MNRAS, 483, 5166
Everhart, E. 1985, in Dynamics of Comets: Their Origin and Evolution, ed. A. Carusi & G. B. Valsecchi (Dordrecht: Kluwer), 185
Farinella, P., Froeschlé, C., Froeschlé, C., et al. 1994, Natur, 371, 314
Festou, M. C., Rickman, H., & West, R. M. 1993, A&ARv, 4, 363
Gladman, B. J., Migliorini, F., Morbidelli, A., et al. 1997, Sci, 277, 197
Gounelle, M., Spurný, P., & Bland, P. A. 2006, M&PS, 41, 135
Granvik, M., Morbidelli, A., Jedicke, R., et al. 2016, Natur, 530, 303
Granvik, M., Morbidelli, A., Jedicke, R., et al. 2018, Icar, 312, 181
Greenstreet, S., Ngo, H., & Gladman, B. 2012, Icar, 217, 355
Gwyn, S. D. J., Hill, N., & Kavelaars, J. J. 2012, PASP, 124, 579
Haack, H., Grau, T., Bischoff, A., et al. 2012, M&PS, 47, 30
Halliday, I., & McIntosh, B. A. 1990, Metic, 25, 339
Hui, M.-T., Ye, Q.-Z., Knight, M., Battams, K., & Clark, D. 2015, ApJ, 813, 73
Jenniskens, P. 2004, AJ, 127, 3018
Jenniskens, P., Fries, M. D., Yin, Q.-Z., et al. 2012, Sci, 338, 1583
Jewitt, D., Asmus, D., Yang, B., & Li, J. 2019, AJ, 157, 193
Jewitt, D., & Li, J. 2010, AJ, 140, 1519
Jones, G. H., Knight, M. M., Battams, K., et al. 2018, SSRv, 214, 20
Jones, J., & Brown, P. 1993, MNRAS, 265, 524
Jones, J., Brown, P. G., Ellis, K. J., et al. 2005, P&SS, 53, 413
Jopek, T. J., Rietmeijer, F. J. M., Watanabe, J., Williams, I. P., et al. 2013, in Proc. Astronomical Conf., Meteoroids 2013, ed. T. J. Jopek, F. J. M. Rietmeijer, J. Watanabe, & I. P. Williams (Poznan: AMU Scientific Publishing House), 371
Kaiser, T. 1960, MNRAS, 121, 284
Kimura, H., Mann, I., Biesecker, D. A., & Jessberger, E. K. 2002, Icar, 159, 529
Knight, M. M., A'Hearn, M. F., Biesecker, D. A., et al. 2010, AJ, 139, 926
Knight, M. M., Fitzsimmons, A., Kelley, M. S. P., & Snodgrass, C. 2016, ApJL, 823, L6
Knight, M. M., & Walsh, K. J. 2013, ApJL, 776, L5
Kreutz, J. 1891, PUSK, 6, 67
Lamy, P., Faury, G., Llebaria, A., et al. 2013, Icar, 226, 1350
Lamy, P. L., Toth, I., Fernandez, Y. R., & Weaver, H. A. 2004, in Comets II, ed. M. C. Festou, H. U. Keller, & H. A. Weaver (Tucson, AZ: Univ. Arizona Press), 223
Lauretta, D. S., Hergenrother, C. W., Chesley, S. R., et al. 2019, Sci, 366, 3544
Mainzer, A., Grav, T., Bauer, J., et al. 2011, ApJ, 743, 156
Marsden, B. G. 1967, AJ, 72, 1170
Masiero, J. R., Mainzer, A. K., Grav, T., et al. 2011, ApJ, 741, 68
Mazur, M., Pokorný, P., Weryk, R. J., et al. 2019, RaSc, submitted

Nishiizumi, K., Caffee, M. W., Hamajima, Y., Reedy, R. C., & Welten, K. C. 2014, M&PS, 49, 2056

Öpik, E. 1951, PRIAA, 54, 165

Pokorný, P., Sarantos, M., & Janches, D. 2018, ApJ, 863, 31

Pokorný, P., Vokrouhlický, D., Nesvorný, D., Campbell-Brown, M., & Brown, P. 2014, ApJ, 789, 25

Scherer, P., & Schultz, L. 2000, M&PS, 35, 145

Sekanina, Z., & Chodas, P. W. 2005, ApJS, 161, 551

Spurný, P., Borovička, J., Mucke, H., & Svoreň, J. 2017, A&A, 605, A68

Tabeshian, M., Wiegert, P., Ye, Q., et al. 2019, AJ, 158, 30

Tedesco, E. F., Williams, J. G., & Matson, D. L. 1989, AJ, 97, 580

Vokrouhlický, D., & Nesvorný, D. 2012, A&A, 541, A109

Webster, A. R., Brown, P. G., Jones, J., Ellis, K. J., & Campbell-Brown, M. 2004, ACP, 4, 1181

Whipple, F. L. 1940, PAPhS, 83, 711

Whipple, F. L. 1951, ApJ, 113, 464

Whipple, F. L. 1983, IAUC, 3881, 1

Whipple, F. L., & Huebner, W. F. 1976, ARA&A, 14, 143

Wiegert, P., & Brown, P. 2005, Icar, 179, 139

Wiegert, P. A. 2015, Icar, 252, 22

Wyatt, S. P., & Whipple, F. L. 1950, ApJ, 111, 134

Ye, Q., Brown, P. G., & Pokorný, P. 2016, MNRAS, 462, 3511

Ye, Q., & Granvik, M. 2019, ApJ, 873, 104

Ye, Q., Wiegert, P. A., & Hui, M.-T. 2018, ApJL, 864, L9

Ye, Q.-Z., Hui, M.-T., Kracht, R., & Wiegert, P. A. 2014, ApJ, 796, 83